Biol. Proced. Online 2005; 7(1): 31-40.
doi:10.1251/bpo103
April 18, 2005

An improved method for constructing and selectively silanizing double-barreled, neutral liquid-carrier, ion-selective microelectrodes

Jason S.T. Deveau[1], Michael I. Lindinger[2]*, Bernard Grodzinski[1]

[1]Department of Plant Agriculture, University of Guelph, Guelph, Ontario, Canada, N1G 2W1.

[2]Department of Human Biology and Nutritional Sciences, University of Guelph, Guelph, Ontario, Canada, N1G 2W1.

*Corresponding Author: M.I. Lindinger, Department of Human Biology and Nutritional Sciences, University of Guelph, Guelph, Ontario, Canada, N1G 2W1. Phone: (519) 824-4120 ext. 53752; Fax: (519) 763-5902; Email: mlinding@uoguelph.ca

Submitted: October 27, 2004; Revised: March 11, 2005; Accepted: March 14, 2005.

Indexing terms: Microelectrode; Ion-Selective Electrodes.

ABSTRACT

We describe an improved, efficient and reliable method for the vapour-phase silanization of multi-barreled, ion-selective microelectrodes of which the silanized barrel(s) are to be filled with neutral liquid ion-exchanger (LIX). The technique employs a metal manifold to exclusively and simultaneously deliver dimethyldichlorosilane to only the ion-selective barrels of several multi-barreled microelectrodes. Compared to previously published methods the technique requires fewer procedural steps, less handling of individual microelectrodes, improved reproducibility of silanization of the selected microelectrode barrels and employs standard borosilicate tubing rather than the less-conventional theta-type glass. The electrodes remain stable for up to 3 weeks after the silanization procedure. The efficacy of a double-barreled electrode containing a proton ionophore in the ion-selective barrel is demonstrated *in situ* in the leaf apoplasm of pea (*Pisum*) and sunflower (*Helianthus*). Individual leaves were penetrated to depth of ~150 μm through the abaxial surface. Microelectrode readings remained stable after multiple impalements without the need for a stabilizing PVC matrix.

INTRODUCTION

Ion-selective microelectrodes (ISMEs) were developed primarily to investigate the activity of specific ions in the inter- (1, 2) and intra-cellular (3) compartments of animals and plants (4). The mV reading obtained from the ion-selective barrel reports the sum of the chemical potential generated by the activity of the selected ion, plus the transmembrane (for intracellular microelectrodes) or total extracellular electrical potential of the fluid being probed. The desired chemical potential is isolated from the net signal by mathematically subtracting the electrical potential reported by the reference barrel or microelectrode (5).

When employing two separate single-barreled microelectrodes (one ion-selective and one reference) it is recognized that the tips may rest in different cellular or extracellular compartments, which contributes to measurement artifacts (6, 7). Also, because each cell is unique, mean values must be used rather than direct measurements and this necessitates several impalements via cumbersome manipulation (8). Furthermore, certain cells are too small or too fragile to accommodate multiple tips. In order to minimize damage and to confirm tip location, combination (i.e. multibarrel) microelectrodes were introduced. For example, the recessed-tip H^+-selective microelectrode (9-11) consists of pulled H^+-selective glass that has been serially fused inside a

standard reference microelectrode. The manufacture of such a microelectrode is complicated and the H^+-selective glass may have an undesirably high electrical resistance (3, 12). Accordingly, many experimenters continued to use single-barreled ion-selective microelectrodes (5, 6, 13, 30) due to the inherent labour and difficulties in producing reliable multi-barrel ISMEs.

Alternatively, multi-barreled microelectrodes have been constructed from pre-fabricated theta-style tubing, which has a continuous septum that creates two distinct channels (14, 15). However, the septum can be compromised during pulling (16), the tubing may not be compatible with conventional halfcell/holders and they require complicated silanization procedures to prevent reference-barrel contamination (3, 15). The issue of controlled silanization of only the internal surface ion-selective barrel(s) is most significant. Inadvertent silanization of the reference barrel results in ion-selective coupling, slower reference-barrel response times and misleading readings. Silanization of the outer surface of the ion-selective barrel (for example using wet silanization) results in reduced hydrophobicity of the external surface, loss of liquid ion exchange resin (LIX), and contamination of the reference barrel. While the silanization of single-barreled microelectrodes is hardly a new technique (17), its application to multi-barrel designs continues to develop.

In the present paper, we detail improvements to the silanization procedure reported by Semb *et al*. (3) for theta style, double-barreled ISMEs. Our technique employs standard borosilicate tubing (18), allowing a conventional halfcell/holder to seal the ion-selective barrel and prevent possible dislocation of the LIX column due to cytosolic (turgor) pressure. The technique provides excellent control over the internal silanization process, excludes silane from the reference barrel without the need for N_2 purging of the reference barrel, minimizes electrode manipulation and makes it possible to silanize several high quality ISMEs simultaneously. Double-barreled H^+-selective microelectrodes created using this technique were characterized in standard buffer solutions and used to measure the *is situ* pH of mesophyll apoplastic space in detached *Pisum* (pea) and *Helianthus* (sunflower) leaves (i.e. the intercellular space between the cells of intact leaves).

MATERIALS AND METHODS

Borosilicate Tubing: Borosilicate tubing with an outer diameter of 1 ± 0.05 mm and an inner diameter of 0.58 ± 0.05 mm (Friedrich & Dimmock, Millville, New Jersey, USA) fits standard halfcell/holders (World Precision Instruments, Sarasota, Florida, USA) and were used to make the ion-selective barrels. Standard borosilicate tubing resists microcracking (which can cause short circuits) and has a softening point conducive to creating desirable tip geometry when heated and pulled (5). The reference barrel was also comprised of borosilicate tubing, but with a slender borosilicate rod fused inside (commonly referred to as omega-dot tubing). The rod creates an acute angle with the inner wall, which promotes capillary action during filling (16, 19).

Construction: Over a Bunsen flame, an 8 cm length of omega-dot tubing was softened at a point ~2.5 cm from the least jagged end and bent to 45° (similar to the technique in Blatt and Slayman; (20)). This "elbow" later serves to separate the distal ends of the two barrels, allowing easy access to either barrel during silanization, back-filling and halfcell/holder mounting (Fig. 1).

An 8 cm length of standard borosilicate tubing was placed parallel to the bent tubing and a 0.75 cm length of common black, irradiated, 3/32" diameter PVC shrink-wrap tubing (Alpha Wire Corporation, Thief River Falls, Minnesota, USA) was slipped over the paired barrels, 2-3 mm from the bend in the reference barrel. This shrink-wrapping process was repeated at the tip of the two barrels. It is important that both barrels be parallel and the segment of shrink-wrap sufficiently long, else shearing tension may change the tip geometry during heating and pulling. Also, the shrink-wrap must not be in contact with the elbow, else torque may be created during heating and pulling. The PVC was heated, allowed to cool and a 1 cm length of coloured, thin-wall, 3/32" diameter polyolefin shrink-wrap (DSG-Canusa, Toronto, Canada) was heated and shrunk over top, ~0.25 cm from the elbow. Later, when the microelectrodes are

baked, this second wrap serves the dual purpose of squeezing the inner layer into closer contact with the borosilicate, and it increases the diameter of the area to allow the micropipette puller improved grip. Unlike fusing (18), or contact cement (8), employing shrink-wrap to construct multi-barrel microelectrodes is fast, easy, reduces the chance of compromises (i.e. cross-talk) between barrels and allows the experimenter to colour-code the microelectrode.

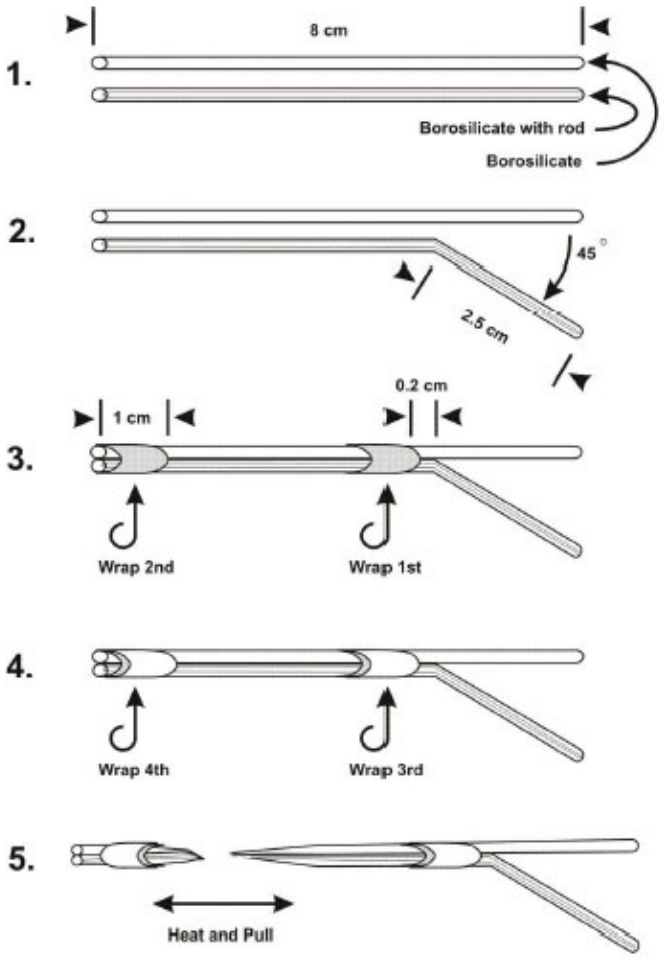

Fig. 1: A five step protocol illustrating the components and construction of a blank, and the resultant double-barreled microelectrode. 1. Two 8 cm sodium borosilicate tubes. The one with a rod (Omega dot glass) becomes the reference barrel, and the one without becomes the ion-selective barrel. **2.** The reference barrel is softened and bent to 45°, 2.5 cm from the end. **3.** 0.75 cm PVC wrap is shrunk 0.2 cm from the elbow, and at the tip. **4.** 1 cm polyolefin wrap is shrunk over the PVC. **5.** The blank is pulled in a micropipette puller.

Pulling Protocol: The intended application of the ISME determines the appropriate pulling protocol and resultant tip geometry. In this case, a double-barrel ISME with a short shank (~60 μm) was required to penetrate the cuticle and epidermal layer of the leaf tissue without breaking (4). The tip was strengthened using a variation of the pull-and-twist protocol described in (8) and is detailed in Table 1. All microelectrodes were forged on a WPI PMP 100 vertical multi-barrel microelectrode puller (World Precision Instruments, Sarasota, Florida, USA). If pulls suddenly began to fail (tips with incorrect configuration), the cause was usually the position of the microelectrode at the heating element. Additionally, the puller was prone to overheating, creating play between the clamps and the microelectrode. The solution was to pull batches of 15 or less electrodes at a time.

Table 1: Pulling protocol program for the WDI PMP-100 multi-barrel micropipette puller. This protocol creates double-barrelled sodium borosilicate microelectrodes with a sharp taper and ~0.5 μm tip diameter.

Step number	Time (s)	Heat level	Circumstance
1	30	90%	Preheating
2	3	90%	Rotate 180°
3	Variable	85%	Pull at 15 psi for 2.5 mm
4	1	0%	Rest
5	12	87%	Preheating
6	Variable	65%	Pull at 15 psi for 20 mm
7	5	0%	Air-cooled

Tip modification: Once pulled, the tip opening of the double-barreled microelectrode was <0.5 μm; this small tip is very thin walled and prone to breaking upon penetration of the leaf. We attempted to enlarge the opening by breaking the tip of the electrode to lower resistance, aid in filling and sharpen the penetrating edges (21). Standard procedural beveling of the tip was attempted (3) using a K.T. Brown-type micropipette beveller (Sutter Instrument Company, Novato, Califronia, USA) while the electrical resistance was monitored. The tip geometry, however, was such that the opening in one barrel was not flush with the other barrel. This meant that one barrel could penetrate a plasma membrane while the other remained in extracellular space, and this could create confounds. Further, the ISME tip could clog with salt crystals from electrolyte originating from the reference barrel even after multiple rinses and >24 hours of soaking (Fig. 2).

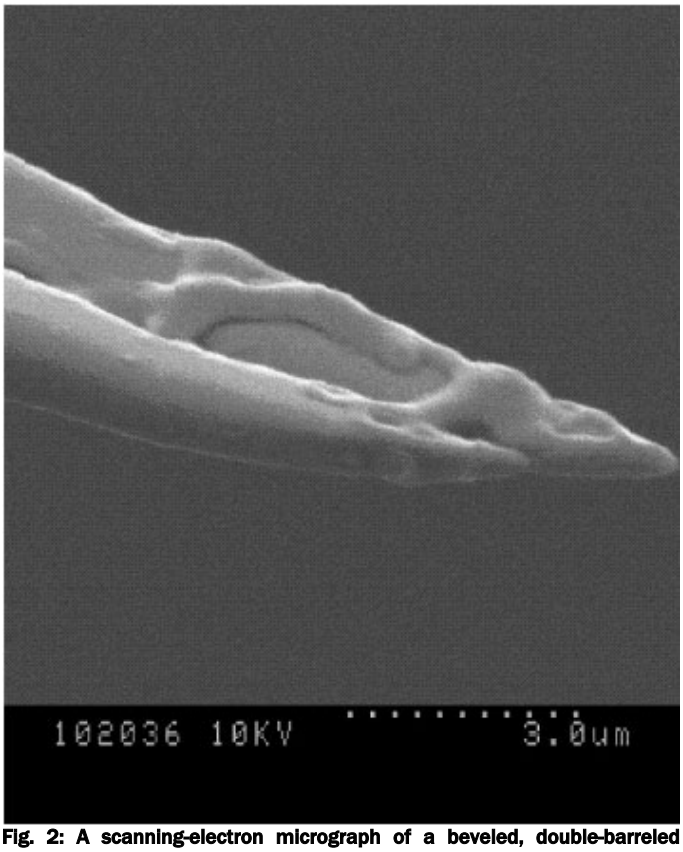

Fig. 2: A scanning-electron micrograph of a beveled, double-barreled microelectrode tip (after gold/palladium sputter-coated) showing accumulation of electrolyte clogging the tip openings. Scale bar is 3.0 µm.

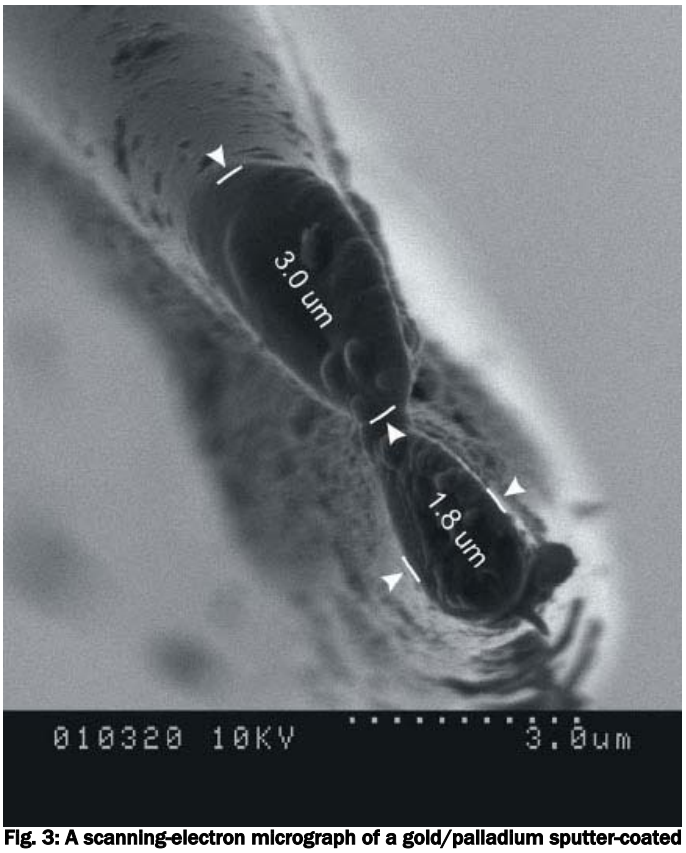

Fig. 3: A scanning-electron micrograph of a gold/palladium sputter-coated double-barreled microelectrode tip. This electrode was emptied using positive pressure, refilled 3 times with ddH_2O, and soaked tip-down for 24 hours in ddH_2O following wet-beveling. Note the persistence of veins of salt crystals coating the tip and shank. Scale bar is 3.0 µm.

Therefore, controlled breaking of the tip proved to be a more desirable method of tip modification. Under a 10x microscope objective, a micromanipulator was used to advance the tip of the microelectrode towards a reflective glass surface, which enabled the operator to judge when the tip made contact (18, 22, 23). By lightly tapping on the microscope stage, the tip was cleanly broken to a larger diameter by sub-micron degrees. Figure 3 is a scanning electron micrograph of a double-barreled microelectrode tip that has been sputter-coated with gold-palladium.

Baking and Silanization: The benefits of silanizing microelectrodes were first reported by Walker (17) and were applied to double-barreled microelectrodes by Lux and Neher (14). Many custom silanization techniques have been reported in response to the inherent difficulties involved in the controlled silanization of the ion selective barrel, while leaving the reference barrel uncontaminated. A barrel cannot be treated before heating and pulling because >99% of the glass in the tip is newly exposed following pulling and would be unsilanized (24).

Our silanization manifold (Fig. 4) is based on the vapour delivery systems described previously (3, 7). It was designed to hold, desiccate and simultaneously silanize five double-barrel ISMEs. Each ion-selective barrel was inserted into manifold ports to create a gas-tight seal around the outside of the barrel. The manifold (with microelectrodes) was baked for one hour at ~180°C to eliminate all moisture and prevent the possible formation of polymeric silicon compounds that readily plug microelectrode tips (8). While still in the oven, 0.5 ml of 5% DMDCS in toluene (Supelco, Bellefonte, Pennsylvania, USA) was injected into the manifold through a septum. Expansion of the heated DMDCS vapor within the manifold chamber forced silane through the ion-selective barrels. The microelectrodes and manifold continued to bake for an additional hour to dissipate the solvent, leaving only the ion-selective barrels hydrophobic.

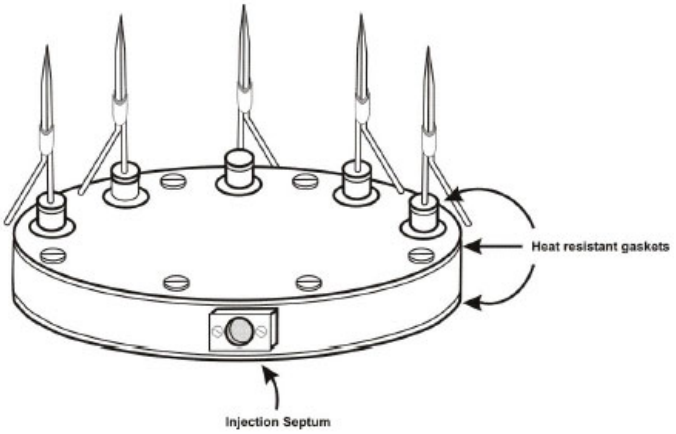

Fig. 4: The silanizing chamber supports multiple double-barreled microelectrodes during desiccation in an oven. It then exposes the collective ion-selective barrels to 0.5 cc's of 5% dimethyldichlorosilane in tetrohydrofuran, introduced through an injection port. Opportunity for accidental breakage is reduced, silanization is reliable, and unintentional contamination of the reference barrel is rare.

The manifold, still holding the microelectrodes, was then placed in a desiccator to cool. Once cool, microelectrodes were removed from the manifold and left in the desiccator for a further 12-24 hours to ensure the complete evaporation of solvent. They could be stored in this fashion for up to three weeks because silanization does not remain a permanent condition.

Filling the Microelectrode: Twenty four hours prior to intended use, silanized DISMs were backfilled with electrolyte solution of pH and composition approximating that of the apoplasm (pH 5.4; 0.5 mM KCl, 0.1 mM NaCl and 0.1 mM $CaCl_2$). The composition of the electrolyte solution was based on (5) and (24) with modification to mimic the composition of apoplasm recovered from several sources (25, 26). We did not buffer the electrolyte solution so as to easily detect electrical potential responses to changes in apoplasm pH, and apoplasm also has a low non-bicarbonate proton buffering capacity.

The flexible 34 AWG Microfil tip (World Precision Instruments, Sarasota, Florida, USA) of a 5cc syringe was inserted to the shoulder of either barrel and the electrolyte solution was back-filled. Fifty psi of positive pressure from a PV830 pneumatic Picopump (World Precision Instruments, Sarasota, Florida, USA) was used to force the solution to the tip of the ion-selective barrel and if necessary, the tip of the reference barrel. If air bubbles were observed, they were dislocated using the syringe, or the microelectrode was held tip-down and tapped lightly with a fingernail until the bubble rose to the shoulder for subsequent displacement using the syringe.

Once both barrels were filled, the ion-selective barrel was prepared to receive a column of liquid ion exchange resin (LIX). A small quantity of proton-selective LIX (95297 H_2 Ionophore II - Cocktail A, Fluka Chemical Corp., Ronkonkoma, New York, USA) was stored in the dark within a 1 mm I.D. glass capillary. For filling the IMSE tip, the LIX capillary was bracketed onto a customized microscope stage under the 10x objective lens. The microelectrode tip was advanced to the LIX and when the tip compromised the meniscus, the LIX would spontaneously flow into the ion-selective barrel. On occasion, if flow did not occur, ~10 psi negative pressure was briefly applied through the stem to initiate filling. Achieving a LIX column of ~1000 μm required 5-10 minutes. Once filled, a brief pulse of positive pressure was issued through the reference barrel to ensure the absence of any contaminating LIX, and the tip was rinsed in dH_2O. This seemingly long column allowed for shrinkage due to LIX drift as it continued to drift back towards the shoulder, coating the interior of the barrel. The final column length following drift and insertion into the modified halfcell/holder (described below) was ~500 μm. LIX column length (and resultant resistance) reportedly has little appreciable effect on response time once it exceeds 200 μm (18). Therefore, the longer column increased the duration of ISME stability without impairing performance.

Assembling the Halfcell/Holder: A chlorided silver wire (a silver wire immersed briefly into household bleach, then rinsed) was inserted into the reference barrel to create the connection with the amplifier. The ion-selective barrel was then inserted into a halfcell/holder (WPI, Sarasota, Florida, USA). To prevent insertion pressure from forcing the LIX from the tip of the microelectrode, the halfcell/holder was modified: a tiny overflow channel was drilled through to the central column. Excess electrolyte was displaced through the overflow channel during insertion and a small amount of putty was used to re-seal the overflow channel. The halfcell/holder was then attached to the headstage and the electrode tip placed into an electrolyte solution for 12-24 hours. This allowed any air bubbles to dissolve and allowed the LIX column to finish drifting in the tip.

Equipment and Calibration: The electrical potential was reported by a Duo 773 Dual Microprobe amplifier (World Precision Instruments, Sarasota, Florida, USA), sampled at 100 Hz and filter decimated to record at 10 Hz by Labview 5.0 (National Instruments, Austin, Texas, USA). The ion-selective input impedance was a standard ~10^{15} Ω and the reference input impedance was a standard ~10^{11} Ω. A MHW-103 hydraulic micromanipulator (Narshige Industries, Tokyo, Japan) positioned the ISME over the stage of a dissection microscope contained within a Faraday cage encased in 1mm square 0.5mm diameter copper wire mesh. The cage itself was located on a vibration-resistant table, in a grounded, vibration-proofed room specially constructed for electrophysiology.

Calibration was performed in 5 ml volumes of phosphate buffer at pH 4.0, 7.0 and 10.0 (Sigma-Aldrich, St. Louis, Montana, USA.) with rinses of dH_2O between buffers. The proton selective LIX reportedly has linear pH-mV response characteristics from pH 4 to 9.5, therefore the pH 10 buffer exceeded this characteristic. Calibration was performed before (pre-experimental calibration) and after (post-experimental calibration) to determine the stability and reliability of the ISME during the experiment. Linear regression analysis of calibration data on pre and post runs were performed and the equations used to calculate pH (and H^+ activity).

Plant preparation: Pea seeds (*Pisum sativum* cv. Improved Laxton's Progress) and sunflower seeds (*Helianthus annus*, cv.) were purchased from Stokes Seeds (St. Catherines, ON, Canada). Peas were planted in 5 inch diameter plastic pots, and sunflowers were planted in 10 inch diameter plastic pots, both filled with Promix BX growth medium. Plants were grown in the greenhouse at 25°C/18°C day/night regime. The duration of the photoperiod was kept at 16 hours with high pressure sodium lamps (430 W Son Agro bulbs, Phillips, Somerset, New Jersey) supplementing natural sunlight from 8am to 12am. Plants were watered every 2-3 days and fertilized every 7-10 days with a 0.25% solution of 20-8-20 (N-P-K) fertilizer. All plants were grown at ambient CO_2 (~350 μl l^{-1}).

Only healthy, mature leaves were used in impalements. 28-35 day old pea plants were flowering, but had no visible fruit. There were ~10 compound leaves per pea plant at this point. The sunflower plants were 43 - 50 days old, were about to flower and had 7-8 opposite leaves per plant. The whole leaf (with petiole) was severed with a razor blade immediately prior to the experiment and quickly transferred to a transparent Perspex vessel. The cut end of the petiole was submerged in a H_2O bath (dechlorinated tap water) and sealed in place by an adjustable collar. The rest of the leaf was supported face-down on the adjacent working surface of the vessel and held in place by a drop of vacuum grease. The vessel was transferred from the greenhouse to the laboratory and was placed on the dissection microscope stage. The microelectrode was arranged over the desired point of impalement and the ground electrode (silver wire, 0.25 mm in diameter, chlorinated by brief immersion in household bleach) was placed in the petiole bath. The total time expired between severing the leaflet and the initial impalement was ~15 minutes.

Impalement: The point of impalement was ~2 mm adjacent to the midvein and ~20 mm from the basal end, on the abaxial surface of the *Helianthus* leaf or *Pisum* leaflet. The microelectrode was advanced ~150-250 μm into the tissue, with the goal of situating the tip in the apoplasm (extracellular fluid) of the spongy mesophyll. The large tip diameter made any stable intracellular impalement unlikely. When the reported potential across the electrode tip suggested a sustainable apoplasmic situation, denoted by an acidic pH ~5.0 - 6.0 and a reference potential of ~0.0 mV (27), the ISME could remain in place for an hour or more. After achieving the desired recording, the ISME was then carefully extracted from the leaf and post-experimental calibration immediately performed.

Calculation of H^+ activity: Data were imported to SYSTAT 8.0 (SPSS, Chicago, Illinois, USA), where steady-state values corresponding to calibration solutions were recorded. Linear regressions were run on calibration results to determine the R^2 values and all mV data was converted to pH using the slope and X intercept ($y = mx + b$). pH values were then exported to EXCEL (Microsoft, USA) where H^+ activity was determined using the dissociation constant of water (K_W) ($pH = -\log_{10}(10^{-7}) = 7$).

RESULTS

Calibration and Effects of Physical Interference: The DISMs demonstrated a near-Nernstian response of 54.0 - 58.0

mV pH^{-1} units during calibration, had less than 5 % overall drift in slope between pre- and post-experimental calibrations, and maintained a stable response rate. During calibration, a stable reference potential was achieved in <1.0 second and the ion-selective potential reached t_{90} in ~8 seconds, which translates to ~25 seconds to reach an average $\Delta E\ \Delta t^{-1}$ of 0.9 mV min^{-1} (28). Pre- and post-experimental calibration results from electrodes used to generate results reported in the present paper, including those used to measure apoplasm pH of detached *Pisum* and *Helianthus* leaves, were similar. Calibration results prior to use were linear (r^2 = 0.992 ± 0.004, slope 55 ± 3 mV.pH^{-1}, n=10); there was no degradation of the linear response after use (r^2 = 0.998 ± 0.002, slope 56 ± 3 mV.pH^{-1}, n = 10). Two-way repeated measures ANOVA with respect to pre- vs post-calibration and calibration buffer showed no difference in response times 1.79 ± 0.35 s (p = 0.670).

The physical manipulations described here are basic proof-of-principle, providing a foundation for ambient conditions surrounding the experiment, specifically the presence of an electrically neutral, vibration proof environment. A double-barreled H^+-selective microelectrode created using our protocol was challenged by vibration, changes in illumination, and current injection. The illumination of the microscope stage was measured using a photosynthetically active radiation meter (Apogee Instruments, Logan, Utah, USA). Ambient light was 3.0 µM $m^{-2}s^{-1}$ and illumination from a Series 180 Fiber-Lite (Dolan-Jenner Industries Inc., Lawrence, MA, USA) was 1250 µM m^{-2} s^{-1}. The temperature of the test solution (19.3°C) was measured using a RTD Digital thermometer (Cole-Palmer, Vernon Hills, Illinois, USA).

Figure 5 is a record of the potentials reported by a proton ISME (pre- and post calibrations are not shown to increase the resolution of the graph). Resistances were determined by injecting current through each barrel; 1 nA = 27 MΩ (range 19-35 MΩ) for reference and 1 pA = 54 GΩ (range 38-56 GΩ) for ion selective. The variation in illumination did not change the temperature of the test solution, or affect the potential reported by the DISM. Minor physical vibration did not affect the potential, but major impacts to the floor caused transient deflections approaching 10 mV. The operator's gross movements also caused minor, transient deflections in potential, but only when the Faraday cage doors were wide open. These data indicate that data obtained from microelectrode measurements will be the result of chemical and biological activity within the sampling solution and are not the result of confounds from physical sources of interference such as light, temperature or gross operator movement.

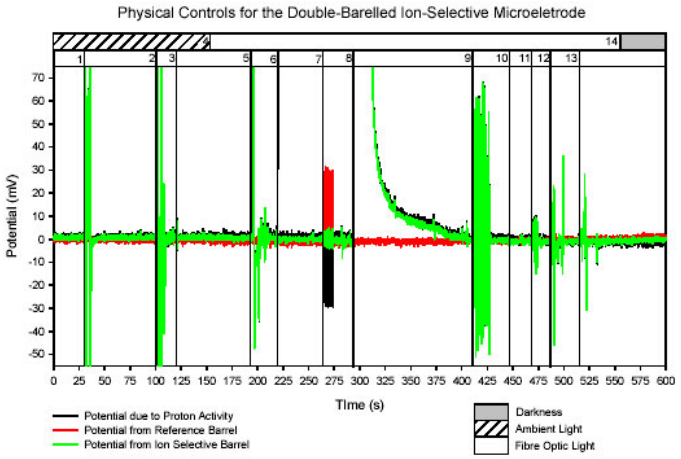

Fig. 5: Physical controls for the double-barreled ion-selective microelectrode. The LISM is in pH 7.0 phosphate buffer. A series of physical challenges are issued to determine the effects on the recorded potential. **1 - 29 sec:** A minor deflection was caused by holding a light meter close to the stage. The operators hand was ~5 cm from the headstage. Ambient room light is 3.0 µM · m^{-2} · s^{-1}. **2 - 101 sec:** A minor deflection was caused by the operator moving close to the Faraday cage as the doors remained open. **3 - 117 sec:** The 2 foot long sensor-wand of the digital thermometer is placed in the test solution. Temperature of 5 ml of buffer is 19.3 °C. **4 - 156 sec:** Fibre optic light source is turned on. **5 - 196 sec:** The operator moves close to the headstage through the open doors. Seconds later 1254 µM · m^{-2} · s^{-1} reported by the light meter. **6 - 220 sec:** Operator, now grounded, moves in front of open Faraday cage. The doors are carefully shut to prevent any more gross operator-based interference. **7 - 264 sec:** 6,1nA pulses are sent through the reference barrel. **8 - 290 sec:** The ion-selective barrel received a burst of alternating current, called a "tickle," which sent the signal off scale. **9 - 411 sec**; Signal returns to scale, and 9 1pA pulses are sent through the ion-selective barrel. **10 - 447 sec:** The closed Faraday cage is lightly physically tapped 5 times by the operator. **11 - 470 sec:** The operator jumps 5 times next to vibration proof table. **12 - 493 sec:** The door to the cage is opened carefully. **13 - 519 sec:** Temperature is measured at 19.3 °C, after >8.5 minutes of illumination. **14 - 558 sec:** All ambient light is turned off, and the incident light from the monitor is not registered by the light meter at the stage. Deflections stem from the operators proximity to the headstage.

Effects of Chemical Interference: To identify any potential ionic interference, a H^+-selective double-barreled microelectrode was subjected to a series of chemical challenges to buffered solutions, as detailed in Figure 6. 20 ml volumes of buffer with different varying pH were mixed by a magnetic stirrer, as 5 ml volumes of potentially competing salt solutions were titrated into each buffer over 30-60 seconds. Linear regression performed on the pre- and post-experimental

calibrations resulted in regression coefficients (R^2) of 0.970 ± 0.012 and 0.975 ± 0.009 and a Nernstian response of 56.6 ± 2.3 mV / pH unit. Based on this relationship, the potentials reported in each buffer corresponded accurately to their known pHs, even when non-phosphate buffers were used. Only the titration of sodium hydroxide into a phosphate buffer slightly (~7 mV) affected the potential due to the decrease in solution H^+ activity.

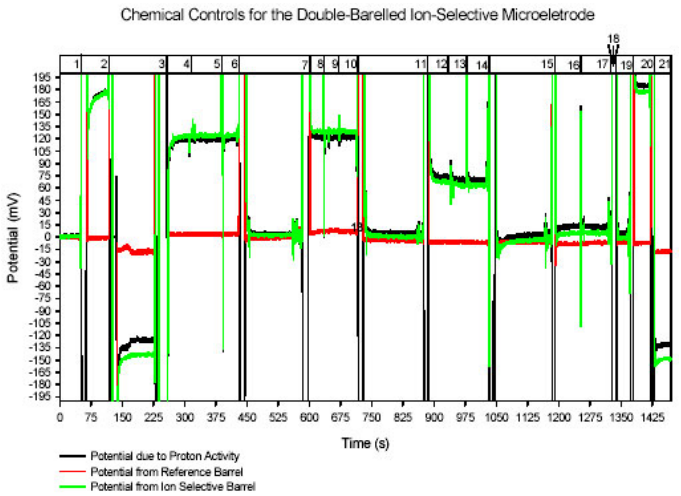

Fig. 6: Chemical controls for the double-barreled ion-selective microelectrode. The LISM begins in pH 7.0 phosphate buffer. A series of chemical challenges are issued to determine the effects on the recorded potential. The stirring plate and bar are on throughout the experiment. **1 - 0 sec:** Commercial pH 7.0 phosphate buffer. **2 - 50 sec:** Commercial pH 4.0 phosphate buffer. **3 - 118 sec:** Commercial pH 10.0 phosphate buffer. **4 - 264 sec**: Placed in 20 ml acetate buffer at pH 5.0. **5 - 314 sec**: Start titrating with potassium phosphate (5 ml) to a total of 5000 µM. **6 - 398 sec:** A small peak as the operator touched the Faraday cage, and titration is complete. **7 - 432 sec**: Commercial pH 7.0 phosphate buffer. **8 - 602 sec**: Placed in 20 ml acetate buffer at pH 5.0. **9 - 644 sec**: Start triturating potassium chloride (5 ml) to a total of 5000 µM. **10 - 680 sec**: A small peak as the operator touched the Faraday cage, and titration is complete. **11 - 716 sec**: Commercial pH 7.0 phosphate buffer. **12 - 888 sec**: Placed in 20 ml citrate buffer at pH 6.0. **13 - 941 sec**: Start titrating with sodium hydroxide (5 ml) to a total of 500 µM. **14 - 980 sec**: A small peak as the operator touched the Faraday cage. **15 - 1030 sec**: Commercial pH 7.0 phosphate buffer. **16 - 1185 sec**: Placed in 20 ml homemade phosphate buffer at pH 7.0. **17 - 1255 sec**: Start titrating with sodium chloride (5 ml) to a total of 500 µM. Small static discharge from operator as titration begins. **18 - 1310 sec**: A small peak as the operator touched the Faraday cage, and titration is complete. **19 - 1335 sec:** Commercial pH 7.0 phosphate buffer. **20 - 1373 sec:** Commercial pH 4.0 phosphate buffer. **21 - 1421 sec:** Commercial pH 10.0 phosphate buffer.

Mesophyll Apoplasm pH measurements: The mesophyll apoplasm pH reported by our ISMEs for *Pisum* was 6.307 (SE ± 0.13 / N=34) and 6.37 (SE ± 0.15 / N=10) for *Helianthus* under conditions when the leaves were illuminated. In these experiments, microelectrodes expressed acceptable regression coefficients and plausible apoplasm pH after multiple uses (up to three impalements per electrode). During calibration, a steady reference potential was achieved in <1 second and the ion-selective potential reached t_{90} in ~8 seconds, which translates to ~30 seconds to reach an average $\Delta E/\Delta t$ of 0.9 mV/min (28). Figure 7 demonstrates that time course of responses recorded using a double barreled, proton selective microelectrode.

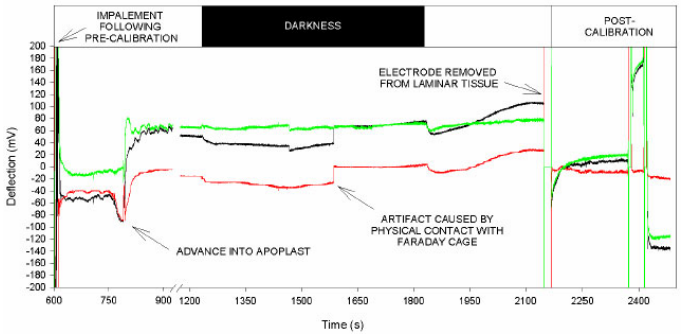

Fig. 7: Apoplasm pH measured in the abaxial surface of a mature, detached leaf of *Hellanthus annus*, with response to darkness and re-illumintion. Onset of darkness and illumination immediately followed by appreciable mV deflection in both reference and ion-selective barrels, translating to a change in apoplasmic proton concentration. **1 - 0 to 250 sec**: Calibration in pH 7.0, pH 4.0 and pH 10.0 phosphate buffers (not shown). **2 - 600 sec**: Electrode tip makes contact with laminar tissue. **3 - 600 to 820 sec**: Microelelectrode tip is advanced ~ 90- microns into tissue. **4 - 820 sec**: Contact is made with the apoplasm in apoplastic free space. **5 - 1250 sec**: Onset of Dark Condition. **6 - 1600 sec**: Artifact caused by contact with Faraday cage. Equal disturbance in both barrels is mathematically cancelled and therefore has no affect on reading of proton concentration. **7 - 1850 sec**: Onset of Light Condition. **8 - 2125 sec**: Microelectrode is back out of the tissue (Circuit broken). **9 - 2175 sec:** Commercial pH 7.0 phosphate buffer. **10 - 2375 sec:** Commercial pH 4.0 phosphate buffer. **11 - 2420 sec:** Commercial pH 10.0 phosphate buffer.

DISCUSSION

The present paper details an improved technique and methodology for obtaining, reliable, reproducible, high quality multi-barrel, ion selective electrodes. In particular, the process for selectively silanizing only the ion-selective barrel of double barreled electrodes is highlighted. The electrodes were capable of being used more than once for successful impalements and measurement of apoplasm pH.

Collectively, >75% of all electrodes constructed (N>200) resulted in successful calibration and measurement of apoplasmic pH. Few authors have published success rates of ISMEs (e.g. 12, 29), but our experience using previously described procedures yielded much lower success. In the present study, ~15% of microelectrodes failed during manufacture, usually during desiccation, tip modification or back-filling. A distinct apoplasmic pH

signal was achieved in ~90% (N>160) of leaf impalements. These ISMEs demonstrated a Nernstian response of 54-58 mV/pH units during calibration, had less than 5% overall drift in slope between pre- and post-experimental calibrations and maintained a reasonably steady pH recording over time. Errors included unresponsive ion-selective barrels, erratic signals (noise), or notably increased response rates. These errors were indicative of an unstable LIX column, likely drifting below 200 μm (18) and were minimized by creating an initially large 1000 μm column and letting the ISME set for an extra 12 hours (totalling ~24h) prior to use. A particularly fast response time was not required to determine steady-state apoplasmic pH and so, while the larger column was acceptable, it could be reduced if required.

The stability of ISMEs was demonstrated by the physical and chemical controls, where variations in light did not affect temperature or the slope of the reported potential. The ISMEs expressed accurate H^+ activities in several buffers of various pH levels and were not affected by the introduction of potentially competing salt solutions, demonstrating a high potentiometric selectivity coefficient for protons over potassium, sodium and chloride. Tip resistances were within published values (7, 18, 20) and a Nernstian response was achieved (28). Silanized, empty ISMEs could be maintained for up to 3 weeks in a desiccator. Completed ISMEs could, on occasion, be used for multiple plant tissue impalements over a 2-3 day period. However, the ease of manufacture makes repeated use unnecessary.

We believe that the methods described herein represent a substantial improvement to the manufacture of consistently high quality ISMEs suitable for extracellular and intracellular studies in plant and animal tissues. The main benefits of this methodology include: selective silianization of only the internal surface of the ion selective barrel, avoiding contamination of the reference barrel and external surface; a strengthened tip created by the joining of two regular sized barrels (as opposed to using theta glass capillaries), which also facilitates filling of the capillaries with electrolyte solution; the production of many electrodes at the same time; and greater than 75% of the manufactured electrodes can be used successfully. Electrodes that have been pulled have small openings (<0.5 μm) that are amenable to for intracellular recordings in animal cells (3). As described herein, these tips can be reproducibly be enlarged in a controlled way so as to facilitate recording in the extracellular space.

Manufacture and Troubleshooting: A web-based appendix has been designed to guide the user in the manufacture, preparation and troubleshooting of ISMEs (link: http://www.uoguelph.ca/hb+ns/MILTroubleshootingGuide.htm). Consultation will hopefully eliminate the need for redundant forensics and assist in the production of sturdy, reliable, and problem-free microelectrodes. The reliability and uncomplicated manufacture of ISMEs based on this protocol could eliminate the continued use of single barreled microelectrodes when measuring ion activities of plant and animal fluids.

ACKNOWLEDGMENTS

This research was supported by NSERC (Natural Science and Engineering Research Council of Canada) and CRESTech (The Centre for Research in Earth and Space Technology).

REFERENCES

1. Hnik P, Holas M, Krekule I, Kuriz N, Mejsnar J, Smiesko V, Ujec E, Vyskocil F. Work-induced potassium changes in skeletal muscle and effluent venous blood assessed by liquid ion-exchanger microelectrodes. *Pflugers Arch* 1976; 362(1):85-94.
2. Vyskocil F, Illes P. Non-quantal release of transmitter at mouse neuromuscular junction and its dependence on the activity of Na^+-K^+ ATP-ase. *Pflugers Arch* 1977; 370(3):295-297.
3. Semb SO, Amundsen B, Sejersted OM. A new improved way of making double-barreled ion-selective micro-electrodes. *Acta Physiol Scand* 1997; 161:1-5.
4. Miller AJ, Cooksen SJ, Smith SJ, Wells DM. The use of microelectrodes to investigate compartmentation and the transport of metabolized inorganic ions in plants. *J Exp Bot* 2001; 52:541-549.
5. Ammann D. Ion-Selective Microelectrodes – Principles, Design and Application. Springer-Verlag, Berlin, Heidelberg, New York, Tokyo, 1986.
6. Felle H. Proton transport and pH control in *Sinapis alba* root hairs: A study caried out with

double-barrelled pH micro-electrodes. *Journal of Experimental Botany* 1987; 38(187):340-354.
7. Voipio J, Pasternack M, MacLeod K. Ion-sensitive microelectrodes In D. Ogden, Ed, Microelectrode Techniques – The Plymouth Workshop Handbook 2nd Ed. Cambridge: The Company of Biologists Ltd.; 1994. pp. 275-316.
8. Zeuthen T. How to make and use double-barrelled ion-selective microelectrodes. *In* E. Boulpaep, G. Giebisch, eds, Current Topics in Membranes and Transport. Vol.13 1980: 31-47.
9. Thomas RC. Intracellular pH of snail neurons measured with new pH-sensitive glass microelectrode. *J Physio* 1974; 238:159-180.
10. Hagberg H, Larsson S, Haljamae H. A new design of double-barrelled microelectrodes for intracellular pH-measurement in vivo. *Acta Physiol Scand* 1983; 118:149-153.
11. Thomas RC. Eccentric double micropipette suitable for both pH_i micro-electrodes and for intracellular iontophoresis. *Proceedings of Physiological Society* 1985; 371: 24P-25P.
12. Ammann D, Lanter F, Steiner RA, Schulthess P, Shijo Y, Simon W. Neutral carrier based hydrogen ion selective microelectrode for extra- and intracellular studies. *Analytical Chemistry* 1981; 53:2267-2269.
13. Felle H, Bertl A. The fabrication of H^+-selective liquid-membrane micro-electrodes for use in plant cells. *J Exp Bot* 1986; 37(182):1416-1428.
14. Lux HD, Neher E. The equilibrium time course of $[K^+]_o$ in cat cortex. *Exp Brain Res* 1973; 17:190-205.
15. Coles JA, Tsacopoulos M. A method of making fine double-barrelled potassium-sensitive micro-electrodes for intracellular recording. *J Physiol* 1977; 270:12p-14p.
16. Brown KT, Flaming DG. Advanced Micropipette Techniques for Cell Physiology. IBRO Handbook Series: Methods in the Neurosciences. Vol. 9. A.D. Smith, Ed, New York: John Wiley & Sons; 1995. pp. 235-256.
17. Walker JL Jr. Ion specific liquid ion exchanger microelectrodes. *Anal Chem* 1971; 43:89A-92A.
18. Ujec E, Keller EEO, Kříž N, Pavlik V, Machek J. Low-impedance, coaxial, ion-selective, double-barrel microelectrodes and their use in biological measurements. *Bioelectrochem Bioenergetics* 1980; 7:363-369.
19. Halliwell JV, Whitaker MJ, Ogden D. Using Microelectrodes In D. Ogden, Ed, Microelectrode Techniques – The Plymouth Workshop Handbook 2nd Ed. Cambridge: The Company of Biologists Ltd.; 1994. pp. 275-316.
20. Blatt MR, Slayman CL. KCl leakage from microelectrodes and its impact on the membrane parameters of a nonexcitable cell. *J Mem Biol* 1983; 72:223-234.
21. Kurkdjian AC, Barbier-Brygoo H. A hydrogen ion-selective liquid-membrane microelectrode for measurement of the vacuolar pH of plant cells in suspension culture. *Analytical Biochemistry* 1983; 132:96-104.
22. Sonnhof U, Forderer R, Schneider W, Kettenmann H. Cell puncturing with a step motor driven manipulator with simultaneous measurement of displacement. *Pflugers Archiv* 1982; 392:295-300.
23. Lowen CZ, Satter RL. Light-promoted changes in apoplastic K^+ activity in the *Samanea saman* pulvinus, monitored with liquid membrane microelectrodes. *Planta* 1989; 179:421-427.
24. Munoz J-L, Deyhimi F, Coles JA. Silanization of glass in the making of ion-sensitive microelectrodes. *J Neurosci Methods* 1983; 8:231-247.
25. Ruan Y-L, Patrick JW, Brady CJ. The composition of apoplast fluid recovered from intact developing tomato fruit. *Austra J Plant Physiol* 1996; 23:9-13.
26. Gabriel R, Schäefer L, Gerlach C, Rausch T, Kesselmeier J. Factors controlling the emissions of volatile organic acids from leaves of *Quercus ilex* (holm oak). *Atmospheric Environment* 1999; 33:1347-1355.
27. Felle H, Hanstein S. The apoplastic pH of the substomatal cavity of *Vicia faba* leaves and its regulation responding to different stress factors. *J Exp Bot* 2002; 53(366):73-82.
28. Buck RP, Lindner E. Recommendations for nomenclature of ion-selective electrodes (IUPAC Recommendations 1994). *Pure and Applied Chemistry* 1994; 66:2528-2536.
29. Felle H. The apoplastic pH of the *Zea mays* root cortex as measured with pH-sensitive microelectrodes: aspects of regulation. *Journal of Experimental Botany* 1998; 49(323):987-995.
30. Hanstein S, Felle HH. The influence of atmospheric NH3 on the apoplastic pH green leaves: a noninvasive approach with pH-sensitive microelectrodes. *New Phytol* 1999; 143:333-338.